Wei *et al.*
European Journal of Medical Research (2024) 29:642
https://doi.org/10.1186/s40001-024-02223-6

European Journal of Medical Research

RESEARCH

Open Access

Distinct phenotypes in the preeclamptic-like mouse model induced by adenovirus carrying sFlt1 and recombinant sFlt1 protein

Yingying Wei[1†], Haojun Tian[1†], Xuancheng Wei[1†], Ai Zhang[2], Mengtian Wei[1], Ruixue Wang[1], Lu Zhang[1], Ping Qiao[3*] and Kai Wang[1*]

Abstract

Background Preeclampsia (PE) is a pregnancy-specific, multisystemic disorder that affects 2–8% pregnancies worldwide and is a leading cause of maternal and perinatal mortality. At present, there is no cure for PE apart from delivery the placenta. Therefore, it is important and urgent to possess a suitable animal model to study the pathology and treatment of PE. When exogenous soluble fms-like tyrosine kinase-1 (sFlt-1) is administered, pregnant animals develop a PE-like phenotype. However, there is no report on the comparison between different methods of constructing PE mouse models using sFlt-1.

Methods In this study, the adenovirus carrying sFlt-1(ADV-Flt-1) and recombinant murine sFlt-1 protein (RM Flt-1) are two different methods were used to induce and compare PE-like mouse models. Pregnancy outcomes were examined on E14.5 and E17.5.

Results Our data showed that on E14.5, the adenovirus carrying sFlt-1 induced PE-like phenotype, whereas recombinant murine sFlt-1 protein not. On E17.5, both the two methods induced PE-like phenotype including hypertension, proteinuria, fetal growth restriction, placental and glomerular endotheliosis. Importantly, in the adenoviral-mediated sFlt-1 group, the circulating concentration of sFlt-1 were higher than in the recombinant sFlt-1 group, leading to earlier and more severe symptoms of PE. The ADV-Flt-1 group is easy to operate, quickly effective and efficient. The RM Flt-1 group is safer and more stable, with good repeatability, but slower to take effect.

Conclusions We proposed that the adenoviral-mediated sFlt-1 model can better simulate early-onset and severe PE.

Keywords Preeclampsia, Adenovirus, Soluble fms-like tyrosine kinase-1, Mice, Model

[†]Yingying Wei, Haojun Tian and Xuancheng Wei have contributed equally to this work.

*Correspondence:
Ping Qiao
zzybbmm@aliyun.com
Kai Wang
wangkevinmd@tongji.edu.cn
[1] Clinical and Translational Research Center, Shanghai Key Laboratory of Maternal Fetal Medicine, Shanghai Institute of Maternal-Fetal Medicine and Gynecologic Oncology, Shanghai First Maternity and Infant Hospital, School of Medicine, Tongji University, Shanghai 200092, China
[2] Fetal Medicine Center, Qingdao Women and Children's Hospital, Qingdao University, Qingdao 266000, China
[3] Department of Obstetrics, Shanghai First Maternity and Infant Hospital, School of Medicine, Tongji University, Shanghai 200092, China

Background

Preeclampsia (PE) is a pregnancy-specific, multisystemic disorder that affects 2%-8% pregnancies worldwide and is a leading cause of maternal and perinatal mortality [1]. PE is characterized by the onset of hypertension, proteinuria, or other end-organ damage after 20 weeks of gestation [2]. While advancements have been made in understanding PE occurrence over the past two decades, the exact pathogenesis remains elusive [3]. Presently, the disease can be understood in terms of endothelial dysfunction in both the placenta and the mother. The pathogenesis of PE can be delineated into two stages: aberrant placentation and the development of maternal symptoms. Genetic, immunological, and other maternal factors cause placental dysfunction (stage I), which in turn triggers the release of antiangiogenic factors like soluble fms-like tyrosine kinase 1 (sFlt-1), soluble endoglin (sEng) and inflammatory mediators that result in PE (stage II) [1, 4]. Notably, these antiangiogenic proteins play a key role in the pathogenesis of maternal disease, offering avenues for novel diagnostic tools such as risk calculators, predictive models and triage methods. Moreover, these antiangiogenic proteins have emerged as promising targets for therapeutic intervention, with ongoing efforts to develop strategies for their inhibition, elimination, and blockade both in vitro and in vivo [5–7].

At present, for women who develop PE, the treatment is primarily symptomatic, and there is no cure apart from delivery the placenta [8]. Thus, there is a critical need for innovative approaches in the treatment of PE. The therapeutic targets of PE can only be identified through the interaction between basic research in animal models and clinical studies in human subjects [9]. However, findings from human studies often cannot establish causal relationships. Furthermore, there are clear legal and ethical constraints on conducting human clinical research that prevent more detailed investigation. In contrast, experimental studies in animal models allow researchers to conduct preliminary investigations. In addition, they also allow researchers to investigate whether specific factors present in PE can trigger hypertension and other symptoms of the disease. Due to legal and ethical constraints, animal models are indispensable for investigating the occurrence of PE. Therefore, it is precious to possess a suitable animal model that can faithfully replicate the pathogenesis of human PE [10]. Up to now, several approaches across multiple species have been used to generate preclinical models of PE. Commonly employed models including the spontaneously occurring animal models of PE [dahl salt-sensitive rat [11], spontaneous hypertension and heart failure (SHHT) rat [12], and BPH/5 mice [13]]; the surgically-induced [the reduced uterine perfusion pressure (RUPP) model [14]; the environmentally-induced [hypoxia [15], high-salt [16], selenium deficiency [17], cadmium toxicity [18]]; the pharmacologically-induced [sFlt-1 [19, 20], N-omega-nitro-L-arginine methyl ester (L-NAME) [21], peroxisome proliferator-activated receptor-γ (PPAR-γ) antagonists [22], suramin [23], homo-cysteine [24], inhibition of heme oxigenase-1 [25], tumor necrosis factor (TNF)-α [26], endothelin-1 [27], phosphatidylserine/phosphatidylcholine microvesicles [28], deoxycorticosterone acetate (DOCA) [29], and bisphenol A [30]]; the immunologically-induced [lipopolysaccharide (LPS) [31], interleukin 17(IL-17) [32], interleukin-11(IL-11) [33], activated Th1 cells [34], Th17 cell [35], and angiotensin II type I receptor (AT1-AA) autoantibody [36]] and genetically modified animal models [Adenoviral induction of elevated sFlt1 [37–39] and hypoxia-inducible factor 1-α (HIF-1α) [40], endothelial nitric oxide synthase 3(NOS3) knockout [41] and STOX1 overexpression mice [42]].

Among the various induction methods, using sFlt-1 to establish an animal model of PE is the most commonly employed approach. SFlt-1, a splice variant of the vascular endothelial growth factor (VEGF) receptor Flt-1, which lacks the transmembrane and cytoplasmic domains, is produced in high quantities by the placenta and released into the maternal circulation [43]. Acting as a strong antagonist of VEGF and placental growth factor (PlGF), sFlt-1 binds to these molecules in the systemic circulation. Elevated levels of circulating sFlt-1 are observed in PE [44, 45] and this increase may occur before the appearance of clinical symptoms [46]. When sFlt-1 is given to nonpregnant and pregnant rats, it induces a condition characterized by hypertension, proteinuria, and glomerular endotheliosis that recapitulates the symptoms of PE in humans [44].

However, there are different methods for elevating sFlt-1 levels in mice and simulating the occurrence of PE. For instance, administered adenovirus carrying sFlt-1 (ADV-Flt-1) [37], and directly infused mice with recombinant murine sFlt-1 protein (RM Flt-1) both can achieve this objective [19, 20]. The question arises as to whether the two approaches are different, and whether they lead to different degrees of disease models in the context of PE animal models. In this study, two approaches are used to construct PE animal models, aiming to find out the differences between the two approaches.

Methods

Animals

All animal studies were reviewed and approved by the Department of Laboratory Animal Science at Tongji University (TJBG11323103). In this experiment, a total of 80 female and 40 male ICR mice aged 8–12 weeks were purchased from Vital River Laboratory Animal Technology

Co., Ltd., Beijing, China. Mice were housed in a uniform temperature and humidity environment with a strict 12-h light–dark cycle, housed separately by sex, and had unrestricted access to food and water. To obtain a consistent and accurate assessment of the gestational age of mouse embryos, male and female (1:2) mice were placed in pairs overnight. The first appearance of a vaginal plug was expressed as embryonic day 0.5 (E0.5). Pregnant mice (n = 64) were randomly divided into 4 groups (n = 16): *A*. Control: E12.5-E17.5, 100 μl sterile normal saline was injected via tail vein every day; *B.* RM Flt-1: E12.5-E17.5, recombinant murine sFlt-1 3.7 μg/kg (in 100 μl sterile saline; R&D Systems, Minneapolis, MN) was injected via tail vein daily; *C.*pcADV-MCS: E8.5, adenovirus carrying mFc (10^9 plaque-forming units in 100 μl; used as a control for the virus) was injected via tail vein; *D.* pcADV-Flt1: E8.5, adenovirus carrying sFlt-1 (10^9 plaque-forming units in 100 μl) was injected via tail vein. The adenovirus has been described elsewhere [47, 48] and was synthesized by OBiO Technology (Shanghai, China). Blood pressures were noninvasively measured on E14.5 and E17.5 using the tail blood volume with a volume pressure recording sensor CODA System (Kent Scientific, Torrington, CT), with 10 min blinded observations recorded. Blood pressure measurements are performed subsequent to the tail vein injection. At E14.5 and E17.5, pregnant mice were anaesthetized with 3% isoflurane inhalation, retroorbital venous plexus blood samples were collected. Then mice were euthanized by cervical dislocation. Fetus, placentas and kidneys were obtained. The blood samples were left at ambient temperature approximately 18 °C, for one hour to facilitate the removal of cells and coagulation factors. This step was followed by centrifugation at 2000*g* for 30 min at 4 °C, as described earlier in protocols [49]. The serum obtained from this process was subsequently divided into portions and stored at − 80 °C until further examination. From E13.5 to E14.5 and E16.5 to E17.5, 24 h urine was collected using metabolic cages. After centrifuging these specimens at 2500*g* for 10 min at 4 °C, they were stored at − 80 °C. Urinary protein levels were assessed using the Urinary protein kit (Jiancheng Bio, Nanjing, China).

Enzyme-linked immunosorbent assays (ELISAs)

For the estimation of mouse sFlt-1 and sEng, ELISAs were conducted (R&D Systems). Initially, the distinct sera samples were diluted at a ratio of 1:50 and 1:30 respectively for sFlt-1and sEng, followed by incubation in a capture antibody pre-coated 96-well plate. The wells were then subjected to washing and subsequent incubation with a horseradish peroxidase-linked secondary antibody. Later, both the substrate and stop solutions were introduced. Using a set wavelength correction of 540 nm, we assessed optical density at 450 nm. Final concentrations were calculated referencing a standard curve derived from respective standard recombinant proteins.

Preparing tissues for histologic examination

Placentas and kidneys were preserved in 4% paraformaldehyde (PFA) for a duration of 48 h, subsequent to which they underwent standard tissue processing. Paraffin-embedded tissues were sectioned into 3-5 μm slices and mounted onto poly-L-lysine-treated slides. Preparatory steps for the tissue sections involved paraffin removal in xylene and subsequent dehydration through a series of alcohol baths. Following preparation, placental slides were subjected to hematoxylin and eosin (H&E) staining. In contrast, kidney tissue slides were stained with H&E, Periodic Acid Schiff (PAS), and Masson stains. The experimenters who conducted histological examinations of the placenta and kidney were blinded to the treatment.

Immunohistochemical (IHC) analysis of mouse placental tissues

Immunohistochemical studies were performed on deparaffinized paraffin sections, which were subsequently immersed in a citrate buffer for antigen retrieval. Following preparation, samples were incubated overnight at 4 °C with a rabbit-derived anti-CD31 polyclonal antibody (1:150 dilution, Abcam, Cambridge, MA). Immune reactions were visualized using the rabbit specific HRP/DAB (ABC) IHC detection kit (Servicebio, Wuhan, China). Vascular density represented by CD31 positive area was ascertained by capturing four random images per tissue section under a 20 × objective with a Nikon inverted microscope. CD31-positive areas within each image were quantified using the ImageJ imaging analysis tool (NIH, Bethesda, MD).

Statistics

All data were expressed as the means ± SEMs. Significant difference was analyzed by GraphPad Prism 9.0 (GraphPad Software, San Diego, CA). One-way ANOVA was performed to examine the differences among multiple groups. A value of $p < 0.05$ was considered significant (see Table 1).

Results

Hypertension and proteinuria

Two animal models of PE were established by injecting adenovirus carrying sFlt-1 (ADV-Flt-1) and recombinant murine sFlt-1 protein (RM Flt-1) into ICR mice at different time points, as depicted in Fig. 1A. Maternal blood pressures and urine protein were measured on E14.5 and E17.5, respectively. ADV-Flt-1 injection on E14.5 caused significant increases in systolic and mean arterial

Table 1 The characteristics of pregnant mice between 4 groups

Characteristics	E14.5 (n = 8)				E17.5 (n = 8)			
	Control	RM Flt-1	pcADV-MCS	pcADV-Flt1	Control	RM Flt-1	pcADV-MCS	pcADV-Flt1
Systolic blood pressure (mmHg)	109 ± 2.82	113 ± 2.55	111 ± 2.32	120 ± 1.78[ac]	109 ± 1.30	117 ± 0.737[a]	110 ± 2.59	124 ± 2.57[ac]
Diastolic blood pressure (mmHg)	75.7 ± 2.00	76.9 ± 2.67	75.1 ± 2.11	81.7 ± 0.97	74.2 ± 1.58	82.7 ± 1.67[a]	75.0 ± 3.21	86.3 ± 1.06[ac]
Mean arterial pressure (mmHg)	86.7 ± 2.00	89.0 ± 1.81	86.9 ± 2.09	94.6 ± 1.06[ac]	86.0 ± 1.14	94.2 ± 1.14[a]	86.8 ± 2.64[b]	98.8 ± 1.20[ac]
Urine protein (mg/24 h)	223 ± 30.2	252 ± 35.4	245 ± 40.5	403 ± 53.6[ac]	289 ± 42.6	478 ± 33.1[a]	250 ± 31.3[b]	586 ± 55.8[ac]
sFlt-1 concentration (ng/ml)	44.2 ± 3.02	42.4 ± 2.06	42.3 ± 5.10	67.7 ± 7.73[abc]	78.4 ± 5.75	141 ± 14.7[a]	71.8 ± 7.49[b]	196 ± 24.1[ac]
sEng concentration (ng/ml)	4.17 ± 0.226	4.12 ± 0.222	4.18 ± 0.165	4.38 ± 0.189	3.49 ± 0.106	3.80 ± 0.211	3.86 ± 1.120	4.01 ± 0.147
Maternal body weight (g)	40.0 ± 0.519	40.0 ± 0.946	40.6 ± 0.849	41.1 ± 0.891	52.3 ± 1.52	51.5 ± 1.18	50.8 ± 1.85	50.1 ± 2.54
Number of fetuses	11.6 ± 0.981	11.3 ± 0.977	11.4 ± 1.44	11.4 ± 0.885	12.1 ± 0.833	12.4 ± 0.460	11.4 ± 1.40	11.1 ± 1.61
Fetal resorption (%)	0.961 ± 0.961	1.04 ± 1.04	1.39 ± 1.39	3.29 ± 1.72	2.10 ± 1.38	5.25 ± 2.93	3.13 ± 3.13	12.3 ± 8.05
Fetus weight (g)	0.312 ± 0.004	0.303 ± 0.003	0.308 ± 0.004	0.281 ± 0.004[abc]	0.963 ± 0.008	0.927 ± 0.009[a]	0.943 ± 0.012	0.889 ± 0.010[abc]
Placenta weight (g)	0.097 ± 0.002	0.093 ± 0.001	0.094 ± 0.002	0.082 ± 0.001[abc]	0.110 ± 0.002	0.104 ± 0.001[a]	0.108 ± 0.002	0.099 ± 0.001[abc]
Fetus height (cm)	1.13 ± 0.009	1.13 ± 0.009	1.13 ± 0.007	1.10 ± 0.009[abc]	1.90 ± 0.014	1.84 ± 0.017[a]	1.88 ± 0.014	1.78 ± 0.015[abc]
Placenta diameter (cm)	0.669 ± 0.006	0.658 ± 0.007	0.662 ± 0.005	0.637 ± 0.006[ac]	0.713 ± 0.005	0.697 ± 0.006	0.715 ± 0.008	0.670 ± 0.007[abc]
Placental area (mm^2)	9.34 ± 0.483	8.90 ± 0.370	8.86 ± 0.396	7.16 ± 0.267[abc]	10.4 ± 0.414	8.66 ± 0.453[a]	10.6 ± 0.545[b]	7.29 ± 0.270[ac]
Ration of La/JZ depth	3.81 ± 0.186	3.48 ± 0.146	3.49 ± 0.273	2.59 ± 0.170[abc]	5.38 ± 0.484	3.81 ± 0.261[a]	4.75 ± 0.351	2.49 ± 0.167[abc]
$CD31^+$ area fraction (%)	25.3 ± 1.37	23.8 ± 0.863	23.4 ± 0.766	18.8 ± 1.57[abc]	27.1 ± 1.50	20.1 ± 1.30[a]	27.0 ± 1.10[b]	15.1 ± 1.13[abc]
Glomerular area (μm^2)	2722 ± 232	3384 ± 222	3216 ± 230	4360 ± 402[ac]	2953 ± 258	4320 ± 378[a]	2849 ± 205[b]	4990 ± 480[ac]
Fibrotic area fraction (%)	17.2 ± 2.98	29.6 ± 2.85	19.0 ± 3.05	33.9 ± 3.67[abc]	17.2 ± 2.98	29.6 ± 2.85[a]	19.0 ± 3.05	33.9 ± 3.67[ac]

All the data are expressed as the means ± SEMs, and the statistical data were analyzed by one-way ANOVA

[a] Different from Control, [b]Different from RM Flt-1, [c]Different from pcADV-MCS ($p < 0.05$)

pressures. However, RM Flt-1 injected mice did not result in changes in blood pressures on E14.5 (Fig. 1B–D). Importantly, systolic blood pressure, diastolic blood pressure and mean arterial pressures were significantly increased in both ADV-Flt-1 and RM Flt-1 groups on E17.5 (Fig. 1B–D). The RM Flt-1 and ADV-Flt-1 groups had significantly higher urinary protein levels on E17.5, and the ADV-Flt -1 group had slightly higher urinary protein levels than RM Flt-1 group, but there was no statistical difference. Notably, only the ADV-Flt-1 group had significantly higher urinary protein levels on E14.5 compared to the other three groups (Fig. 1E).

Maternal serum concentrations of sFlt-1 and sEng

The serum levels of sFlt-1 in ADV-Flt-1 group significantly increased on E14.5 while this elevation was not observed in the RM Flt-1 group (Fig. 1F). On E17.5, ADV-Flt-1 and RM Flt-1 groups had higher concentration of sFlt-1 than control groups (Fig. 1F). Importantly, serum sFlt-1 in ADV-Flt-1 mice was higher than in RM Flt-1 mice on E17.5, but there was no significant difference. However, sFlt-1 administration did not affect sEng level (Fig. 1G).

(See figure on next page.)

Fig. 1 PE-like mice induced by sFlt-1 injection. **A** Experimental arrangement. Four groups were created by randomizing pregnant mice on E14.5 (n = 32) and E17.5 (n = 32). The following groups were defined: *A*. Control: E12.5–E17.5, 100 µl sterile normal saline was injected via tail vein daily; *B*. RM Flt-1: E12.5–E17.5, recombinant murine sFlt-1(3.7 µg/kg; 100 µl) was injected via tail vein daily; *C*.pcADV-MCS: E8.5, adenovirus carrying mFc (10^9 plaque-forming units in 100 µl) was injected via tail vein; *D*. pcADV-Flt1: E8.5, adenovirus carrying sFlt-1 (10^9 plaque-forming units in 100 µl) was injected via tail vein. **B** Systolic blood pressure in each group at E14.5 (n = 8) and E17.5 (n = 8). **C** Diastolic blood pressure in each group at E14.5 (n = 8) and E17.5 (n = 8). **D** Mean arterial pressure in each group at E14.5 (n = 8) and E17.5 (n = 8). **E** Urine protein of each group at E14.5 (n = 8) and E17.5(n = 8). **F** Serum sFlt-1 concentration in each group at E14.5 (n = 8) and E17.5 (n = 8). **G** Serum sEng concentration in each group at E14.5 (n = 8) and E17.5 (n = 8). Data are means ± SEMs one-way ANOVA, *P < 0.05, **P < 0.01, ***P < 0.001, ****P < 0.0001

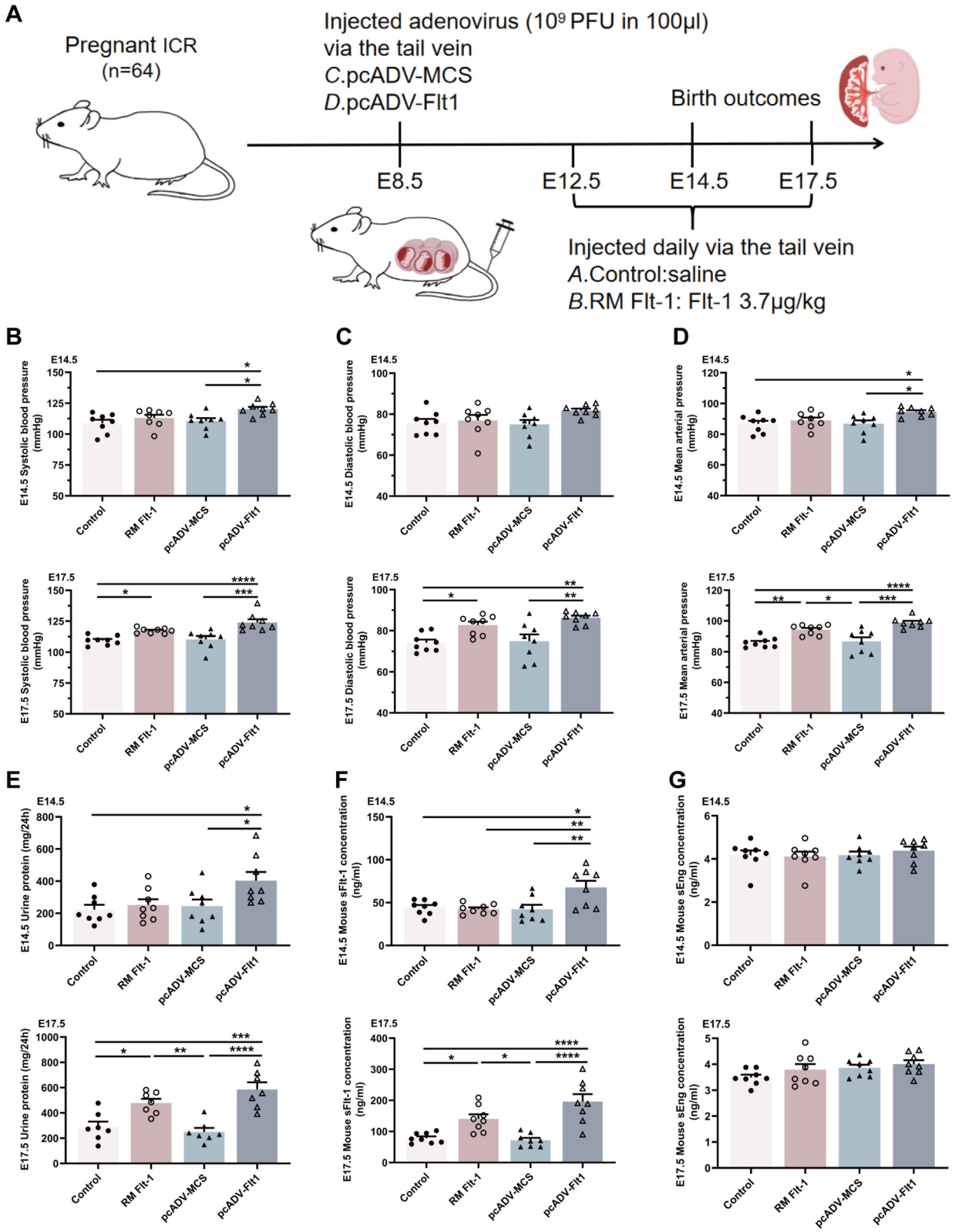

Fig. 1 (See legend on previous page.)

Pregnancy outcome

The occurrence of PE is closely associated with adverse pregnancy outcome, such as restricted intrauterine growth restriction [4]. There was no significant change in maternal body weight (Fig. 2A), number of fetuses (Fig. 2B) and fetal resorption rate (Fig. 2C) between the four groups. It was evident that on E17.5, both the ADV-Flt-1 group and RM Flt-1 group exhibited smaller fetal weight, placental weight, fetal height and placental diameter compared to the control groups. However, only the ADV-Flt-1 group showed reduced fetus and placenta growth on E14.5 (Fig. 2D–H). Notably, the growth restriction of fetus and placenta on E17.5 was more severe in the ADV-Flt-1 group than in the RM Flt-1 group.

Placental pathology

One of the key characteristics of PE is impaired placental vascular development [39, 50]. Accordingly, we scrutinized the histological features of the placentas, focusing on the labyrinth (La) and junctional zone (JZ) via H&E and CD31 IHC staining (Fig. 3A). Remarkably, a noticeable reduction in the overall area of the placental longitudinal section and the thickness ratio of La to JZ layer was found in the ADV-Flt-1 group on E14.5 (Fig. 3B, C). These significant decreases were also found in both RM Flt-1 group and ADV-Flt-1 on E17.5 (Fig. 3B, C). We evaluated placental vascularization using CD31 IHC staining. A significant decrease in placental vessel density and the area fraction of CD31 positive were noted in the ADV-Flt-1 group on E14.5 compared to the others (Fig. 3D, E). Additionally, both RM Flt-1 group and ADV-Flt-1 group on E17.5 showed significant reduction in placental vascularization. More importantly, the defective placental vascular development in ADV-Flt-1 group was more serious than RM Flt-1 group on E17.5. No differences were detected in the control groups.

Renal pathology

Representative kidney images after H&E, PAS and Masson staining showed that the ADV-Flt-1 group on E14.5 led to an increase in the size of the glomeruli, a narrowing of the gap between the visceral and parietal layers, endothelial cell swelling and capillary lumen occlusion, as well as an increase in fibrotic deposits compared to other three groups (Fig. 4). These renal histological alterations resembled the characteristic features of PE [51]. As illustrated in the Fig. 4A2–C2, the kidney pathological damage was observed in both RM Flt-1 group and ADV-Flt-1 group on E17.5. The damage in the ADV-Flt-1 group was slightly more severe than that in the RM Flt-1 group on E17.5; however, the differences were not statistically significant.

Discussion

PE is a complicated, multi-organ disorder related to pregnancy [52]. Over the last ten years, there have been significant advancements in our knowledge of the pathogenesis of PE. While the exact causes of PE are still unclear, recent research indicates that an abundance of circulating anti-angiogenic factors connect the placental dysfunction and the maternal systemic symptoms. This discovery could have significant implications for the treatment and management of PE [53]. Further research is necessary to better understand the expression of these factors and regulate the development of placental vasculature in normal pregnancy and PE, as well as the mechanisms of the maternal response. The understanding of the pathophysiology mechanisms underlying PE has been advanced through a combination of basic research in animal models and clinical research in human subjects [9]. Animal studies have played a crucial role not only in enhancing our understanding of the pathophysiology of PE, but also in identifying potential new treatment options for the disease. Various animal models have been developed to investigate the complex mechanisms involved in PE. It is important to note that in any PE model, the animals are manipulated through surgical, pharmacological, or genetic means to exhibit the relevant features. Additionally, some animal models focus on specific characteristic or factors involved in the progression of PE. Although preclinical models have played a crucial role in elucidating the significance of specific factors in the pathophysiological of PE, it is essential to recognize that PE is a complex, multiorgan disease that initially arises from abnormalities in spiral artery remodeling and placental development.

The sFlt-1 overexpression model has been utilized for testing several new therapies, including VEGF [54] and pravastatin [55]. Given that clinical studies have shown

(See figure on next page.)

Fig. 2 Pregnancy outcomes in sFlt-1 injection mice. **A** Maternal body weight of each group at E14.5 (n = 8) and E17.5 (n = 8). **B** Number of fetuses in each group at E14.5 (n = 8) and E17.5 (n = 8). **C** Fetal resorption of each group at E14.5 (n = 8) and E17.5 (n = 8). **D** Representative images of an fetus and placenta morphology in each group at E14.5 and E17.5. **E** Fetal weights in each group at E14.5 and E17.5. **F** Placenta weight in each group at E14.5 and E17.5 **G** Fetus height in each group at E14.5and E17.5. **H** Placenta diameter in each group at E14.5 and E17.5. Data are means ± SEMs, one-way ANOVA, *P < 0.05, **P < 0.01, ****P < 0.0001

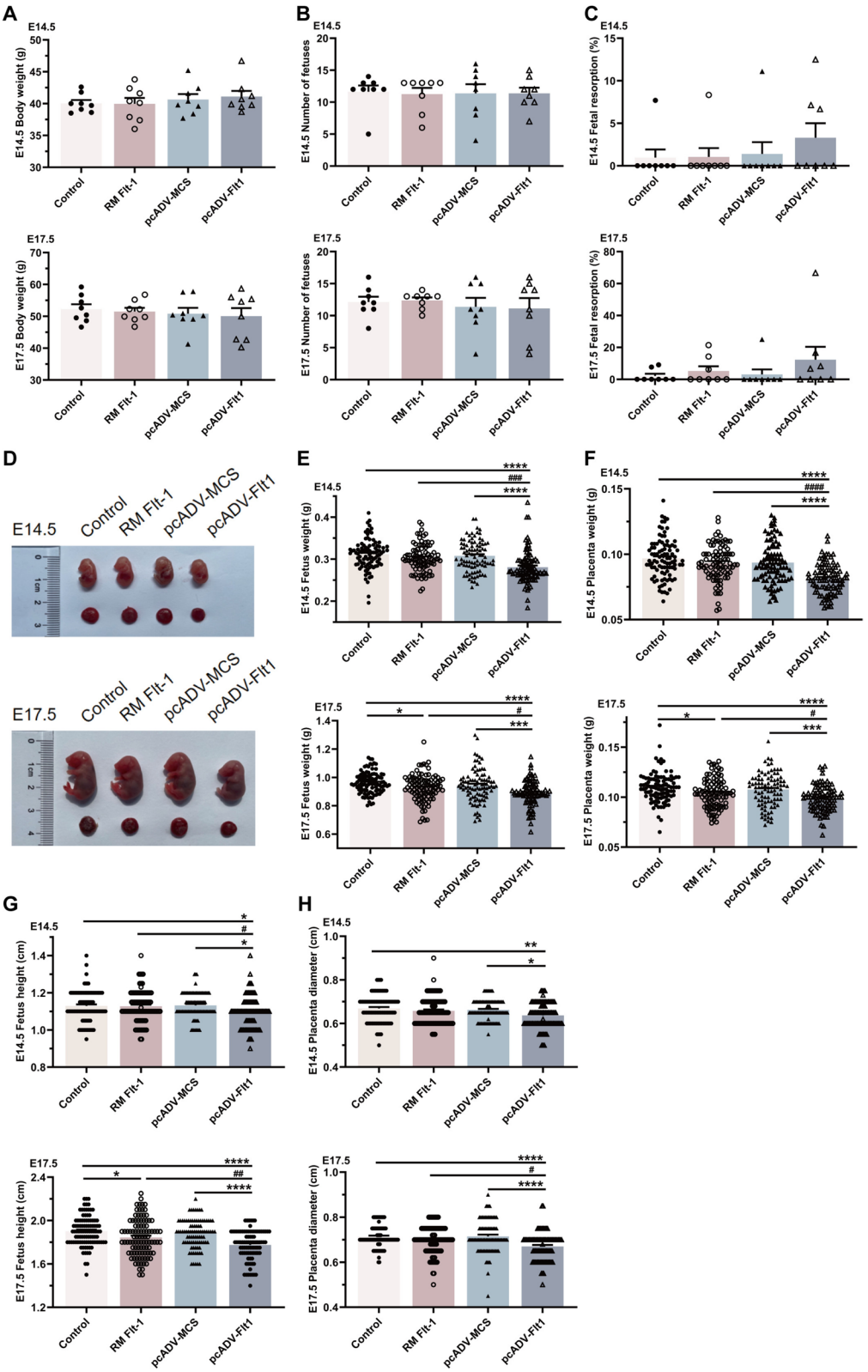

Fig. 2 (See legend on previous page.)

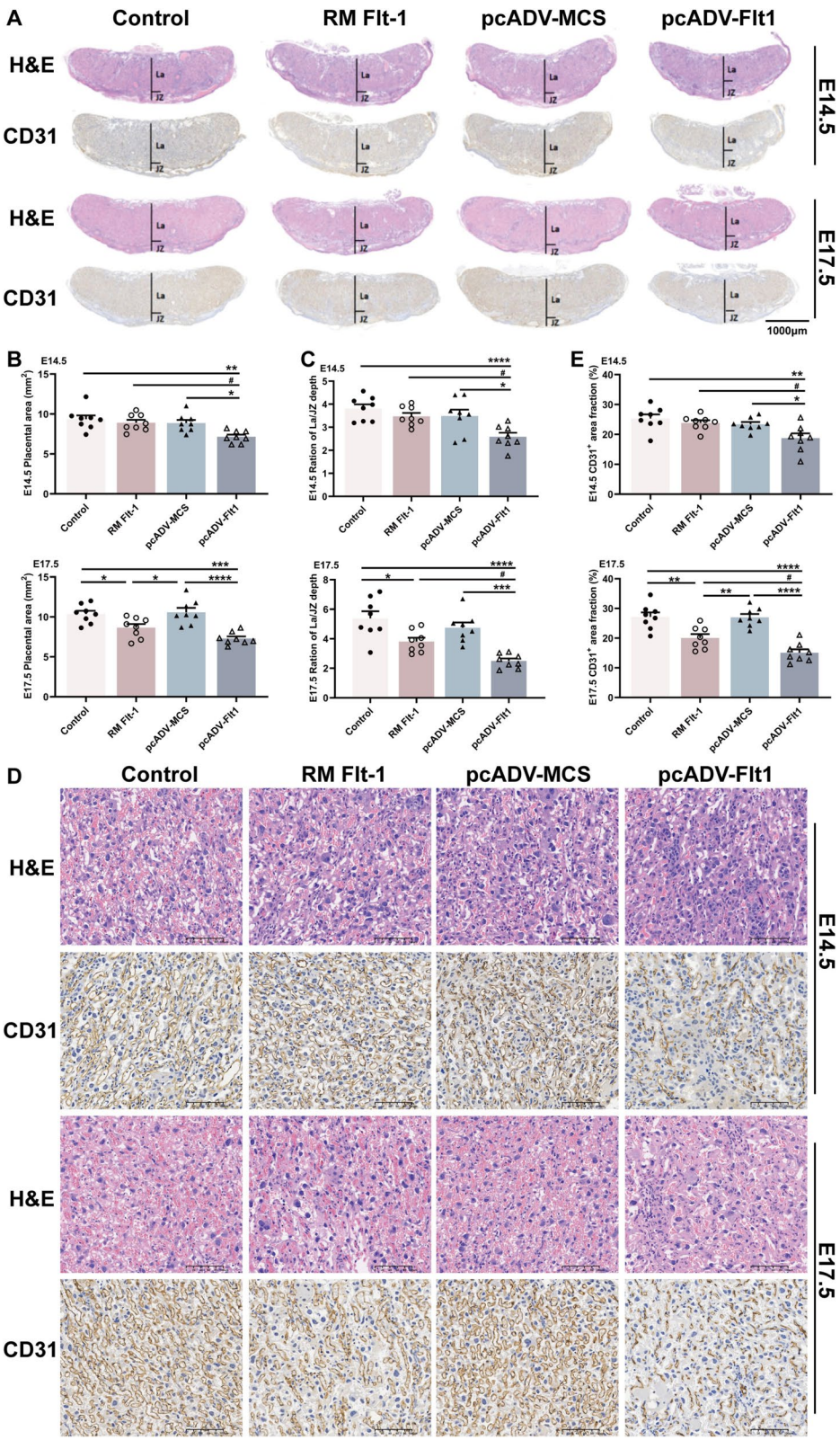

Fig. 3 (See legend on next page.)

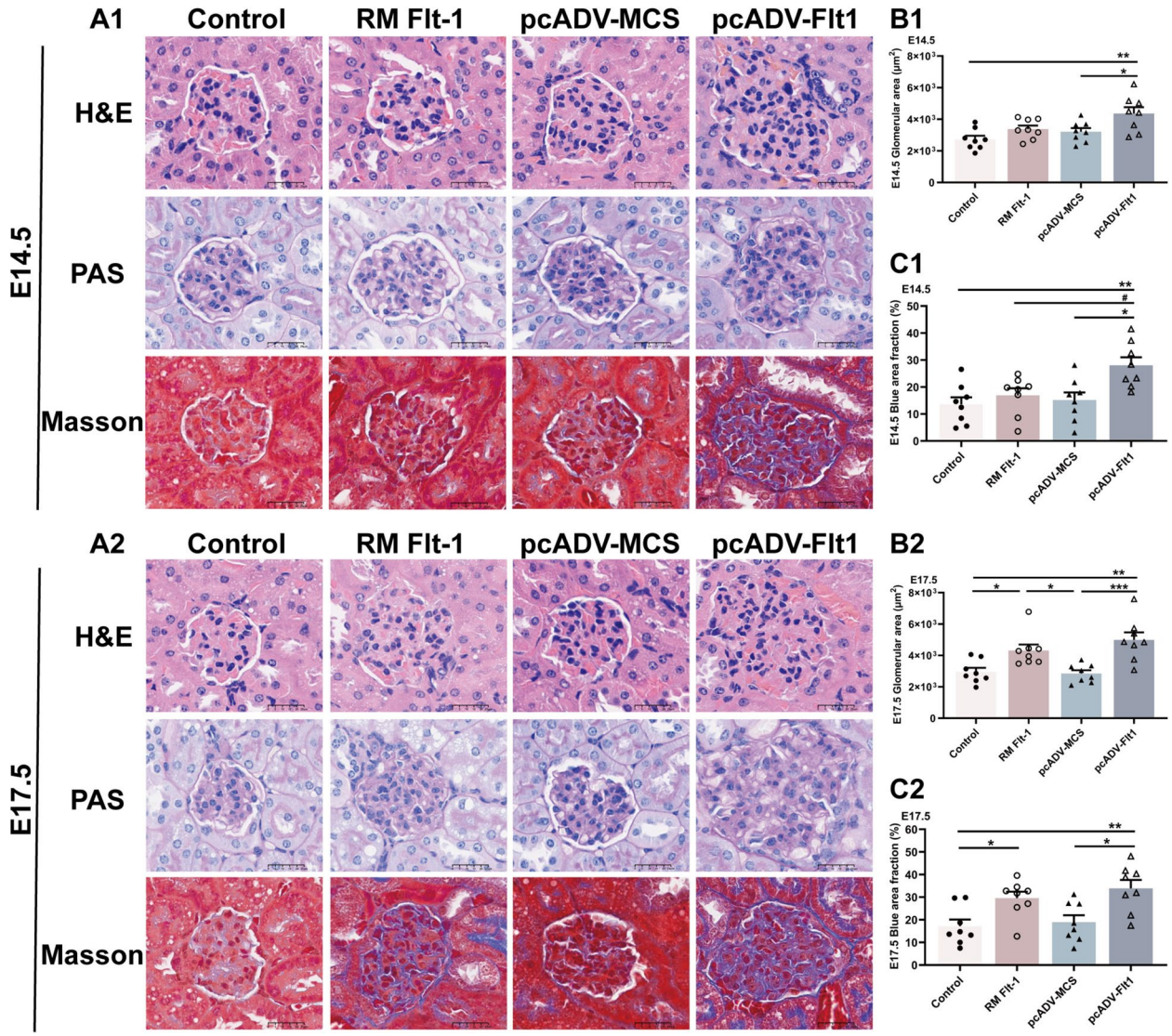

Fig. 4 Renal histopathology in sFlt-1 injection mice. **A** H&E, PAS, and Masson staining representative images of kidney sections in each group at E14.5 (A1, n = 8) and E17.5 (A2, n = 8). Fibrosis deposition is indicated by the color blue in Masson staining, scale bar: 25 μm. **B** Glomerular area in each group at E14.5 (B1, n = 8) and E17.5 (B2, n = 8). **C** Area fraction of glomerular fibrosis in each group at E14.5 (C1, n = 8) and E17.5 (C2, n = 8). Data are means ± SEMs, one-way ANOVA, *P < 0.05, **P < 0.01, ***P < 0.001

that elevated levels of circulating sFlt-1 and decreased PlGF are commonly found in cases of PE, and that an imbalance in angiogenesis factors is linked to adverse maternal and fetal outcomes associated with PE [44–46]. This has generated significant interest in using the sFlt-1 model for testing new therapies and exploring the mechanisms by which sFlt-1 contributes to vascular disease. In our present study, administration of sFlt-1 to pregnant

(See figure on previous page.)

Fig. 3 Placental histopathology in sFlt-1 injection mice. **A** Placental tissue of mice subjected to H&E and CD31 IHC staining (La, labyrinth; JZ, junctional zone), scale bar: 1000 μm. **B** Cross-sectional placental area in each group at E14.5 (n = 8) and E17.5 (n = 8). **C** The depth ratio of the placental labyrinth to junction zone of placenta in each group at E14.5 (n = 8) and E17.5 (n = 8). **D** H&E and CD31 IHC stained representative images of placental tissues at E14.5 and E17.5. Brown color signifies CD31 positive staining, scale bar: 100 μm. **E** Vessel density in the placental labyrinth was determined in each group at E14.5 (n = 8) and E17.5 (n = 8). Data are means ± SEMs, one-way ANOVA, *P < 0.05, **P < 0.01, ***P < 0.001, ****P < 0.0001

mice, with the goal of inhibiting angiogenesis to cause pathophysiological changes, leading to the manifestation of several key characteristics of PE such as hypertension, proteinuria, intrauterine growth restriction, placental and glomerular endotheliosis, which is consistent with previous studies. Although the administration of sFlt-1 can effectively induce a preeclamptic-like mouse model, there are significant differences in placental structure and genomics between mouse and human placentas. More importantly, the shallow implantation of mouse trophoblast cells and limited the role in the arterial remodeling process [56], which is a key mechanism in the pathogenesis of PE. Consequently, the utility of the sFlt-1-induced model for studying trophoblast invasion and vascular remodeling in PE is quite limited. Nevertheless, this model does successfully illustrate the impaired vascularization and angiogenesis characteristic of PE, serving as a valuable reference for research into the prevention or treatment strategies for PE, particularly in the angiogenic therapies.

The main finding of this study was that the differences in the pregnant mice response to sFlt-1 between the RM Flt-1 and ADV-Flt-1 groups. Both the two groups induced PE-like symptoms in pregnant mice, where the ADV-Flt-1 group caused earlier and more elevation of sFlt-1 in maternal sera, which leads to more severe intrauterine growth restriction and placental angiogenesis disorders. In terms of experimental procedures, adenovirus groups can be administered as a single injection into pregnant mice at E8.5, which is simple and convenient, and has fast effect and high efficiency. However, the construction of adenoviruses is time-consuming and costly, and adenoviruses have strong immunogenicity, requiring strict dosage control to prevent immune response. On the other hand, the recombinant sFlt-1 protein has mature stability and safety as a commercial reagent, and has good repeatability for animal experiments. However, this method required six consecutive days of injections from E12.5 to E17.5. At the same time, we found no significant differences in maternal symptoms and pregnancy outcomes between the Control and ADV-MCS groups, suggesting that 100 μL of control saline administered via the tail vein over six consecutive days (E12.5 to E17.5) and a single injection of control adenovirus (10^9 plaque-forming units in 100 μl) did not affect the normal course of pregnancy. To our knowledge, this is the first time to compare the animal models of PE induced by sFlt-1 using different modalities. Therefore, our research provides a good theoretical guide for selecting a suitable PE-like mouse model according to the subject design.

Conclusions

In summary, our study demonstrated that both ADV-Flt-1 and RM-Flt-1 induced preeclamptic mice model successfully. The ADV-Flt-1 group is easy to operate, quick to take effect, and highly efficient. The RM Flt-1 group is safer and more stable, with good repeatability. The key discovery in this study is that ADV-Flt-1 might be a better animal model for early-onset and severe PE. Future work is needed to determine the different effects of sFlt-1 treatment on immune responses and later cardiovascular outcome in both mother and fetus between the two approaches.

Abbreviations

PE	Preeclampsia
sFlt-1	Soluble fms-like tyrosine kinase-1
ADV-Flt-1	Adenovirus carrying sFlt-1
RM Flt-1	Recombinant murine sFlt-1
sEng	Soluble endoglin
VEGF	Vascular endothelial growth factor
PlGF	Placental growth factor
ELISAs	Enzyme-linked immunosorbent assays

Acknowledgements

Not applicable.

Author contributions

Kai Wang: Writing-review & editing, Funding acquisition, Supervision, Conceptualization. Yingying Wei: Writing-Original Draft, Project Administration. Haojun Tian: Methodology, Project Administration. Xuancheng Wei: Software, Project Administration. Ai Zhang and Lu Zhang: Validation. Ruixue Wang: Formal Analysis. Mengtian Wei: Methodology. Ping Qiao: Supervision, Conceptualization. All authors read and approved the final manuscript.

Funding

This work was supported by the National Natural Science Foundation of China (No. 82471720 to Kai Wang), the Shanghai Science and Technology Commission Innovation Plan (201409004500 to Kai Wang), the National Key Research and Development Program of China (No. 2022YFC2704703 to Kai Wang).

Data availability

No datasets were generated or analysed during the current study.

Declarations

Ethics approval and consent to participate

This project was conducted in accordance with animal protocol procedures approved by the Ethics Committee of Department of Laboratory Animal Science at Tongji University (TJBG11323103).

Consent for publication

Not applicable.

Competing interests

The authors declare no competing interests.

Received: 9 July 2024 Accepted: 15 December 2024
Published online: 31 December 2024

References

1. Ives CW, Sinkey R, Rajapreyar I, Tita ATN, Oparil S. Preeclampsia-pathophysiology and clinical presentations: JACC state-of-the-art review. J Am Coll Cardiol. 2020;76(14):1690–702.

2. Obstetricians ACo, Gynecologists. Hypertension in pregnancy. Report of the American College of obstetricians and gynecologists' task force on hypertension in pregnancy. Obstet Gynecol. 2013;122(5):1122–31.
3. Karumanchi SA. Angiogenic factors in preeclampsia: from diagnosis to therapy. Hypertension. 2016;67(6):1072–9.
4. Rana S, Lemoine E, Granger JP, Karumanchi SA. Preeclampsia: pathophysiology, challenges, and perspectives. Circ Res. 2019;124(7):1094–112.
5. Hod T, Cerdeira AS, Karumanchi SA. Molecular mechanisms of preeclampsia. Cold Spring Harb Perspect Med. 2015;5(10): a023473.
6. Romero R, Chaiworapongsa T. Preeclampsia: a link between trophoblast dysregulation and an antiangiogenic state. J Clin Invest. 2013;123(7):2775–7.
7. Levine RJ, Lam C, Qian C, Yu KF, Maynard SE, Sachs BP, et al. Soluble endoglin and other circulating antiangiogenic factors in preeclampsia. N Engl J Med. 2006;355(10):992–1005.
8. Gatford KL, Andraweera PH, Roberts CT, Care AS. Animal models of preeclampsia: causes, consequences, and interventions. Hypertension. 2020;75(6):1363–81.
9. Bakrania BA, George EM, Granger JP. Animal models of preeclampsia: investigating pathophysiology and therapeutic targets. Am J Obstet Gynecol. 2022;226(2S):S973–87.
10. Sakowicz A, Bralewska M, Kamola P, Pietrucha T. Reliability of rodent and rabbit models in preeclampsia research. Int J Mol Sci. 2022;23(22):14344.
11. Gillis EE, Mooney JN, Garrett MR, Granger JP, Sasser JM. Sildenafil treatment ameliorates the maternal syndrome of preeclampsia and rescues fetal growth in the dahl salt-sensitive rat. Hypertension. 2016;67(3):647–53.
12. Sharkey LC, Kirchain S, McCune SA, Simpson GI, Archambault EZ, Boatright NK, et al. Progesterone increases blood pressure in spontaneous gestational hypertension in rats. Am J Hypertens. 2005;18(1):36–43.
13. Davisson RL, Hoffmann DS, Butz GM, Aldape G, Schlager G, Merrill DC, et al. Discovery of a spontaneous genetic mouse model of preeclampsia. Hypertension. 2002;39(2 Pt 2):337–42.
14. Crews JK, Herrington JN, Granger JP, Khalil RA. Decreased endothelium-dependent vascular relaxation during reduction of uterine perfusion pressure in pregnant rat. Hypertension. 2000;35(1 Pt 2):367–72.
15. Wang Z, Huang Z, Lu G, Lin L, Ferrari M. Hypoxia during pregnancy in rats leads to early morphological changes of atherosclerosis in adult offspring. Am J Physiol Heart Circ Physiol. 2009;296(5):H1321–8.
16. Beausejour A, Auger K, St-Louis J, Brochu M. High-sodium intake prevents pregnancy-induced decrease of blood pressure in the rat. Am J Physiol Heart Circ Physiol. 2003;285(1):H375–83.
17. Vanderlelie J, Venardos K, Perkins AV. Selenium deficiency as a model of experimental pre-eclampsia in rats. Reproduction. 2004;128(5):635–41.
18. Zhang X, Xu Z, Lin F, Wang F, Ye D, Huang Y. Increased oxidative DNA damage in placenta contributes to cadmium-induced preeclamptic conditions in rat. Biol Trace Elem Res. 2016;170(1):119–27.
19. Bridges JP, Gilbert JS, Colson D, Gilbert SA, Dukes MP, Ryan MJ, et al. Oxidative stress contributes to soluble fms-like tyrosine kinase-1 induced vascular dysfunction in pregnant rats. Am J Hypertens. 2009;22(5):564–8.
20. Murphy SR, LaMarca B, Cockrell K, Arany M, Granger JP. L-arginine supplementation abolishes the blood pressure and endothelin response to chronic increases in plasma sFlt-1 in pregnant rats. Am J Physiol Regul Integr Comp Physiol. 2012;302(2):R259–63.
21. Herraiz S, Pellicer B, Serra V, Cauli O, Cortijo J, Felipo V, et al. Sildenafil citrate improves perinatal outcome in fetuses from pre-eclamptic rats. BJOG. 2012;119(11):1394–402.
22. McCarthy FP, Drewlo S, English FA, Kingdom J, Johns EJ, Kenny LC, et al. Evidence implicating peroxisome proliferator-activated receptor-gamma in the pathogenesis of preeclampsia. Hypertension. 2011;58(5):882–7.
23. Nash P, Wentzel P, Lindeberg S, Naessen T, Jansson L, Olovsson M, et al. Placental dysfunction in suramin-treated rats–a new model for pre-eclampsia. Placenta. 2005;26(5):410–8.
24. Xu X, Yang XY, He BW, Yang WJ, Cheng WW. Placental NRP1 and VEGF expression in pre-eclamptic women and in a homocysteine-treated mouse model of pre-eclampsia. Eur J Obstet Gynecol Reprod Biol. 2016;196:69–75.
25. George EM, Hosick PA, Stec DE, Granger JP. Heme oxygenase inhibition increases blood pressure in pregnant rats. Am J Hypertens. 2013;26(7):924–30.
26. LaMarca BB, Bennett WA, Alexander BT, Cockrell K, Granger JP. Hypertension produced by reductions in uterine perfusion in the pregnant rat: role of tumor necrosis factor-alpha. Hypertension. 2005;46(4):1022–5.
27. McElvy S, Greenberg SG, Mershon JL, Yang DS, Magill C, Clark KE. Mechanism of uterine vascular refractoriness to endothelin-1 in pregnant sheep. Am J Physiol Heart Circ Physiol. 2001;281(2):H804–12.
28. Omatsu K, Kobayashi T, Murakami Y, Suzuki M, Ohashi R, Sugimura M, et al. Phosphatidylserine/phosphatidylcholine microvesicles can induce preeclampsia-like changes in pregnant mice. Semin Thromb Hemost. 2005;31(3):314–20.
29. Mitchell BM, Cook LG, Danchuk S, Puschett JB. Uncoupled endothelial nitric oxide synthase and oxidative stress in a rat model of pregnancy-induced hypertension. Am J Hypertens. 2007;20(12):1297–304.
30. Ye Y, Tang Y, Xiong Y, Feng L, Li X. Bisphenol A exposure alters placentation and causes preeclampsia-like features in pregnant mice involved in reprogramming of DNA methylation of WNT2. FASEB J. 2019;33(2):2732–42.
31. Xue P, Zheng M, Gong P, Lin C, Zhou J, Li Y, et al. Single administration of ultra-low-dose lipopolysaccharide in rat early pregnancy induces TLR4 activation in the placenta contributing to preeclampsia. PLoS ONE. 2015;10(4): e0124001.
32. Travis OK, White D, Pierce WA, Ge Y, Stubbs CY, Spradley FT, et al. Chronic infusion of interleukin-17 promotes hypertension, activation of cytolytic natural killer cells, and vascular dysfunction in pregnant rats. Physiol Rep. 2019;7(7): e14038.
33. Winship AL, Koga K, Menkhorst E, Van Sinderen M, Rainczuk K, Nagai M, et al. Interleukin-11 alters placentation and causes preeclampsia features in mice. Proc Natl Acad Sci U S A. 2015;112(52):15928–33.
34. Zenclussen AC, Fest S, Joachim R, Klapp BF, Arck PC. Introducing a mouse model for pre-eclampsia: adoptive transfer of activated Th1 cells leads to pre-eclampsia-like symptoms exclusively in pregnant mice. Eur J Immunol. 2004;34(2):377–87.
35. Shields CA, McCalmon M, Ibrahim T, White DL, Williams JM, LaMarca B, et al. Placental ischemia-stimulated T-helper 17 cells induce preeclampsia-associated cytolytic natural killer cells during pregnancy. Am J Physiol Regul Integr Comp Physiol. 2018;315(2):R336–43.
36. Wang HP, Zhang WH, Wang XF, Zhu J, Zheng YQ, Xia Q, et al. Exposure to AT1 receptor autoantibodies during pregnancy increases susceptibility of the maternal heart to postpartum ischemia-reperfusion injury in rats. Int J Mol Sci. 2014;15(7):11495–509.
37. Sato E, Tsunokuni Y, Kaneko M, Saigusa D, Saito R, Shimma S, et al. Metabolomics of a mouse model of preeclampsia induced by overexpressing soluble fms-like tyrosine kinase 1. Biochem Biophys Res Commun. 2020;527(4):1064–71.
38. Carver AR, Tamayo E, Perez-Polo JR, Saade GR, Hankins GD, Costantine MM. The effect of maternal pravastatin therapy on adverse sensorimotor outcomes of the offspring in a murine model of preeclampsia. Int J Dev Neurosci. 2014;33:33–40.
39. Burke SD, Zsengeller ZK, Khankin EV, Lo AS, Rajakumar A, DuPont JJ, et al. Soluble fms-like tyrosine kinase 1 promotes angiotensin II sensitivity in preeclampsia. J Clin Invest. 2016;126(7):2561–74.
40. Tal R, Shaish A, Barshack I, Polak-Charcon S, Afek A, Volkov A, et al. Effects of hypoxia-inducible factor-1alpha overexpression in pregnant mice: possible implications for preeclampsia and intrauterine growth restriction. Am J Pathol. 2010;177(6):2950–62.
41. Pallares P, Gonzalez-Bulnes A. Intrauterine growth retardation in endothelial nitric oxide synthase-deficient mice is established from early stages of pregnancy. Biol Reprod. 2008;78(6):1002–6.
42. Doridot L, Passet B, Mehats C, Rigourd V, Barbaux S, Ducat A, et al. Preeclampsia-like symptoms induced in mice by fetoplacental expression of STOX1 are reversed by aspirin treatment. Hypertension. 2013;61(3):662–8.
43. Clark DE, Smith SK, He Y, Day KA, Licence DR, Corps AN, et al. A vascular endothelial growth factor antagonist is produced by the human placenta and released into the maternal circulation. Biol Reprod. 1998;59(6):1540–8.
44. Maynard SE, Min JY, Merchan J, Lim KH, Li J, Mondal S, et al. Excess placental soluble fms-like tyrosine kinase 1 (sFlt1) may contribute to endothelial dysfunction, hypertension, and proteinuria in preeclampsia. J Clin Invest. 2003;111(5):649–58.
45. Koga K, Osuga Y, Yoshino O, Hirota Y, Ruimeng X, Hirata T, et al. Elevated serum soluble vascular endothelial growth factor receptor 1

(sVEGFR-1) levels in women with preeclampsia. J Clin Endocrinol Metab. 2003;88(5):2348–51.
46. Levine RJ, Maynard SE, Qian C, Lim KH, England LJ, Yu KF, et al. Circulating angiogenic factors and the risk of preeclampsia. N Engl J Med. 2004;350(7):672–83.
47. Lu F, Longo M, Tamayo E, Maner W, Al-Hendy A, Anderson GD, et al. The effect of over-expression of sFlt-1 on blood pressure and the occurrence of other manifestations of preeclampsia in unrestrained conscious pregnant mice. Am J Obstet Gynecol. 2007;196(4):396 e1-7 (**discussion e7**).
48. Lu F, Bytautiene E, Tamayo E, Gamble P, Anderson GD, Hankins GD, et al. Gender-specific effect of overexpression of sFlt-1 in pregnant mice on fetal programming of blood pressure in the offspring later in life. Am J Obstet Gynecol. 2007;197(4):418 e1-5.
49. Jia L, Zhou X, Huang X, Xu X, Jia Y, Wu Y, et al. Maternal and umbilical cord serum-derived exosomes enhance endothelial cell proliferation and migration. FASEB J. 2018;32(8):4534–43.
50. Rai A, Cross JC. Development of the hemochorial maternal vascular spaces in the placenta through endothelial and vasculogenic mimicry. Dev Biol. 2014;387(2):131–41.
51. Lopes van Balen VA, Spaan JJ, Cornelis T, Spaanderman ME. Prevalence of chronic kidney disease after preeclampsia. J Nephrol. 2017;30(3):403–9.
52. Chappell LC, Cluver CA, Kingdom J, Tong S. Pre-eclampsia. Lancet. 2021;398(10297):341–54.
53. Dimitriadis E, Rolnik DL, Zhou W, Estrada-Gutierrez G, Koga K, Francisco RPV, et al. Pre-eclampsia. Nat Rev Dis Primers. 2023;9(1):8.
54. Bergmann A, Ahmad S, Cudmore M, Gruber AD, Wittschen P, Lindenmaier W, et al. Reduction of circulating soluble Flt-1 alleviates preeclampsia-like symptoms in a mouse model. J Cell Mol Med. 2010;14(6B):1857–67.
55. Kumasawa K, Ikawa M, Kidoya H, Hasuwa H, Saito-Fujita T, Morioka Y, et al. Pravastatin induces placental growth factor (PGF) and ameliorates preeclampsia in a mouse model. Proc Natl Acad Sci U S A. 2011;108(4):1451–5.
56. Carter AM. Animal models of human placentation—a review. Placenta. 2007;28(1):41–7.

Publisher's Note